Published in final edited form as:
*Stem Cells*. 2014 April ; 32(4): 983–997. doi:10.1002/stem.1619.

# Neoplastic Reprogramming of Patient-Derived Adipose Stem Cells by Prostate Cancer Cell-Associated Exosomes

**Zakaria Y. Abd Elmageed**[1,*], **Yijun Yang**[1,*], **Raju Thomas**[1,4], **Manish Ranjan**[1], **Debasis Mondal**[2,4], **Krzysztof Moroz**[3,4], **Zhide Fang**[5], **Bashir M. Rezk**[1], **Krishnarao Moparty**[1,6], **Suresh C. Sikka**[1,2], **Oliver Sartor**[1,4], and **Asim B. Abdel-Mageed**[1,2,4,**]

[1]Department of Urology, Tulane University Health Sciences Center, New Orleans, Louisiana, USA, 70112

[2]Department of Pharmacology, Tulane University Health Sciences Center, New Orleans, Louisiana, USA, 70112

[3]Department of Pathology, Tulane University Health Sciences Center, New Orleans, Louisiana, USA, 70112

[4]Tulane Cancer Center, Tulane University Health Sciences Center, New Orleans, Louisiana, USA, 70112

[5]Biostatistics Program, School of Public Health, Louisiana State University Health Sciences Center, New Orleans, Louisiana, USA, 70112

[6]Department of Urology, Southeast Louisiana Veterans Health Care System, New Orleans, Louisiana, USA 70112

## Abstract

Emerging evidence suggests that mesenchymal stem cells (MSCs) are often recruited to tumor sites but their functional significance in tumor growth and disease progression remains elusive. Herein we report that prostate cancer (PC) cell microenvironment subverts PC patient adipose-derived stem cells (pASCs) to undergo neoplastic transformation. Unlike normal ASCs, the pASCs primed with PC cell conditioned media (CM) formed prostate-like neoplastic lesions *in vivo* and reproduced aggressive tumors in secondary recipients. The pASC tumors acquired cytogenetic aberrations and mesenchymal-to-epithelial transition (MET) and expressed epithelial, neoplastic, and vasculogenic markers reminiscent of molecular features of PC tumor xenografts. Our mechanistic studies revealed that PC cell-derived exosomes are sufficient to recapitulate formation of prostate tumorigenic mimicry generated by CM-primed pASCs *in vivo*. In addition to down-regulation of the large tumor suppressor homolog2 (Lats2) and the programmed cell death

**Corresponding author information**: Asim B. Abdel-Mageed, DVM, Ph.D., Department of Urology, SL-42, Tulane University Health Sciences Center, 1430 Tulane Ave, New Orleans, LA 70112, Tel: 504-988-3634, Fax: 504-988-5059, amageed@tulane.edu.
*Z. Y. A. and Y.Y. contributed equally to this work.

**Author contributions**
ABA conceived the study; ZYA, YY, MR, BMR performed the experiments; RT, KM, DM, SCS, OS supplied clinical samples and contributed to the discussion; KM pathology work; ZF statistical analysis; ABA, ZYA analyzed the data, wrote, reviewed and edited the final version of the manuscript.

**DISCLOSURE of POTENTIAL CONFLICTS of INTREST**
The authors declare no conflict of interest.

protein 4 (PDCD4), a neoplastic transformation inhibitor, the tumorigenic reprogramming of pASCs was associated with trafficking by PC cell-derived exosomes of oncogenic factors, including H-*ras* and K-*ras* transcripts, oncomiRNAs miR-125b, miR-130b, and miR-155 as well as the Ras superfamily of GTPases Rab1a, Rab1b, and Rab11a. Our findings implicate a new role for PC cell-derived exosomes in clonal expansion of tumors through neoplastic reprogramming of tumor tropic ASCs in cancer patients.

### Keywords

Prostate cancer; patient ASCs; tumor mimicry; exosomes; oncomiRNAs

## INTRODUCTION

Androgen-deprivation therapy has been the mainstay for treatment of metastatic PC. Although initially effective, molecular mechanisms underlying progression to castration-resistant PC (CRPC) remain elusive [1]. However, there appears to be a crucial link between adiposity and PC progression; Body Mass Index (BMI)>28 kg/cm$^2$ is linked to risk of progression to CRPC, metastasis and death [2]. The adipose-tissue derived stem cells (ASCs) dwell within the perivascular niche of fat tissue and can be isolated from a heterogeneous cell population by differential adhesion of collagenase-digested stromal vascular fraction (SVF). The ASCs have been shown to exhibit stable growth and proliferation kinetics and are amenable in their differentiation repertoire into multiple cell lineages [3]. We have previously demonstrated that these traits make them attractive in regenerative and reparative medicine [4]; however, their safe clinical utility still remains a matter of conjecture [5]. This may be attributed to their potential tumor promoting ability [5] and speculation that epithelial cancers may originate from tissue-specific stem cells or recruitment of cells of non-epithelial origin [6].

Emerging evidence demonstrates that the mean frequencies of blood circulating progenitor cells are significantly higher in obese (BMI ≥30kg/m$^2$) than lean cancer patients or obese controls [7], suggesting that their trafficking from white adipose tissue may represent one of the mechanistic links between adiposity and cancer progression. Indeed, there is mounting realization that MSCs migrate to tumor sites [8] and upon their recruitment may either inhibit or promote tumor growth, primarily through regulated exchange of exosomes, microRNAs, or induction of neovascularization [9]. However, promotion of tumor growth and disease progression through neoplastic transformation of MSCs has not been explored.

Exosomes, small (30–100 nm) extracellular membrane-enclosed vesicles, originate from the endosomal compartment of virtually all cells under normal and disease conditions [10]. Exosome production is tightly controlled by several cytosolic regulatory mechanisms, including elements of the endosomal sorting complex required for transport (ESCRT) and Rab proteins. Besides retaining their distinctive structural features, exosomes express an array of surface markers and harbor contents indicative of their cellular source derivation [11]. A number of the pleiotropic effects of exosomes have been implicated in cell communications and modulation of cell biology [12], primarily due to trafficking of

genomic and proteomic materials into target recipient cells [13]. Although cancer cell-associated exosomes are implicated in tumor growth [11] and metastasis [14], their potential role in neoplastic transformation of tumor tropic MSCs cells has not been elucidated.

MicroRNAs are a class of evolutionarily conserved noncoding single-stranded RNAs that regulate gene expression at the post-transcriptional level through translation inhibition and chromatin-induced silencing mechanisms [15]. The miRNA signatures of exosomes parallel profiles of the originating tumor cells [16]. Recent evidence indicates that dysregulated miRNAs play a central role in tumor initiation, progression, and metastasis by promoting aberrant transcription of oncogenes [17] or tumor suppressors [18]. However, the underlying mechanisms that govern delivery of oncomiRNAs to recipient cells in the tumor microenvironment, especially to the recruited MSCs, are unknown.

In this study we demonstrate, for the first time, that tumor-tropic patient derived ASCs primed with PC cell-derived CM or exosomes undergo genetic instability, mesenchymal-to-epithelial transition (MET), oncogenic transformation, and develop prostate tumors *in vivo*. The oncogenic transformation is associated with down-regulation of the tumor suppressors, Lats2 and PDCD4, upon delivery into pASCs by PC-derived exosomes of oncogenic *ras* transcripts (H-*ras* and K-*ras*), Rab proteins (Rab1a, Rab1b, Rab11a), and oncogenic miRNAs (miR-125b, miR-130b, and miR-155).

## MATERIALS AND METHODS

### Study Population and Fat Tissue Procurement

Based on approved institutional review board (IRB) protocol, intra-abdominal adipose tissue was procured from the space of Retzius near the dome of the bladder from PC patients undergoing radical prostatectomy at Tulane University Hospital and Clinics, New Orleans, LA. Fat tissue was collected from at least sixteen PC patients with a mean preoperative prostate specific antigen (PSA) of 10.5 ng/ml, an average age of 59.5 years, an average Gleason score of 7.2 and an average BMI of 32.4 (Supporting information Table S1). Normal adipose tissue derived stem cells (nASCs) were generously provided by Dr. Jeffery M. Gimble (Pennington Biomedical Research Center, Baton Rouge, LA).

### pASCs Isolation and Culture

The ASCs were isolated from PC patients (pASCs) as we previously described [4]. Briefly, fresh fat tissue (~ 1 gm) was collected, washed three times in phosphate buffered saline (PBS), minced on ice into ~ 1 $mm^3$ pieces. The minced tissue was suspended in 2 mg/ml of collagenase type-I (GIBCO, Invitrogen, Carlsbad, CA) dissolved in PBS containing 5 mM calcium chloride and subsequently incubated at 37°C in a shaking water bath for 2 hr. To remove tissue debris, the cell suspension was successively filtered through 70 and 40 μm cell strainers (BD Biosciences, MD). Mature adipocytes were removed by centrifugation (1,500*g* for 10 min). To remove red blood cells (RBCs), the resulting stromal vascular fraction (SVF) pellet was resuspended and incubated for 2 min in lysis solution (0.15 M ammonium chloride, 10mM potassium bicarbonate and 0.1 mM EDTA). Stem cells were washed in 2 ml 1% bovine serum albumin (BSA) (Sigma-Aldrich, St. Louis, MO),

resuspended in DMEM/F12 medium (1:1; v/v) supplemented with 10% FBS and 1% antibiotics-antimycotic solution (penicillin G, streptomycin and amphotericin B) (Mediatech, Herndon, VA (http://www.cellgro.com)) and maintained at 37°C in an air incubator supplied with 5% $CO_2$.

### Flow Cytometry

The purity of isolated nASCs and pASCs was verified by FACS analysis as previously described [4]. Briefly, cells ($2 \times 10^6$) were aliquoted, resuspended in 1 ml of PBS and incubated in the dark for 20 min at room temperature with one of the following antibodies: CD44-allophycocyanin (APC) and CD29-phycoerythrin-Cy5 (PE-Cy5) (BD Biosciences, San Jose, CA), CD90-PE-Cy5, CD105-PE, CD34-PE, CD45-PE-Cy7, CD79a-PE-Cy5, CD11b-PE-Cy5 (Beckman Coulter, Inc., Brea, CA) and CD326-PE (eBioscience, Inc., San Diego, CA). One cell aliquot was used as an isotype control IgG1/IgG2a and another was unstained. To assess MET, PC cells and single cell suspension of pASC tumor cells, generated *in vivo* by PC cell-derived CM or exosomes, were double stained for either CD44 or pan-cytokeratin. Briefly, cells were initially stained with CD44-APC antibody (BD Bioscience, San Jose, CA) for 15 min. After washing in PBS, the cells were permeabilized by Intraprep-permeabilization reagent according to the manufacturer's instructions (Beckman Coulter, Inc., Brea, CA). After washing, cells were stained with pan-cytokeratin-PE (C11)antibody (Cell Signaling Technology Inc., Danvers, MA) for 15 min. All cells were washed three times in PBS and resuspended in 0.5 ml PBS, vortexed, and analyzed by a Beckman-Coulter Galios 2 Laser, 8 channel flow cytometer running Galios software for acquisition (Center for Stem Cell Research and Regenerative Medicine, Tulane University, New Orleans, LA).

### Enrichment of Tumor-Tropic ASCs

Normal ASCs (nASCs) and pASCs populations with high tropism towards bone metastatic PC cells (C4-2B and PC-3) were enriched using an *in vitro* trans-endothelial migration (TEM) system. The human bone marrow endothelial cell (hBMEC-1) barrier (kindly provided by Dr. Graça D. Almeida-Porada, University of Nevada, Reno, NV) was cultured onto Matrigel™- coated membrane inserts (8 μm pore size) in 12-well plates to generate a confluent hBMEC-1 barrier on the upper chamber. The permeability of the microvessel barrier was checked with Evans blue dye by colorimetric assays. The CM of the PC cells was added to the lower chamber. ASCs ($1 \times 10^5$) were added onto the microvessel barrier and allowed to migrate towards the CM in the lower chamber for 48 h. Only ASC isolates with tropism towards PC CM were propagated (passage <3), stored, and used in subsequent experiments.

### Migration and Cell Surface Marker Expression

Tumor tropic nASCs and pASCs were transduced with a lentivirus construct (Lentifect™) expressing a cytomegalovirus (CMV)-driven green fluorescent protein (pLV-eGFP) according to the manufacturer's protocol (GeneCopoeia, Rockville, MD (http://www.genecopoeia.com)). Using a trans- endothelial migration system, the differential migration of pASCs and nASCs towards CM of PC and normal prostate epithelial

(RWPE-1) cells was investigated for 24 h as described [19]. All experiments were performed in cells cultured in quadruplicates. The eGFP fluorescence was measured at 485/520 nm, respectively, by a fluorescence microplate reader (BIO-TEK Instruments, Winooski, VT (http://www.biotek.com)). In another set of experiments, differences in expression of 89 cell surface marker genes associated with adhesion and invasion ability between migrating and non-migrating pASCs was examined in triplicate by RT2 Profiler custom PCR array according to the manufacturer's recommendation (SA Biosciences, Valencia, CA (http://www.sabiosciences.com)). The results are expressed as Mean ± SEM of three independent experiments.

## Animal Studies

Six-week-old athymic nude (*nu/nu*) male mice (NCI, Frederick, MD) were housed in a pathogen-free facility with free access to commercial rodent chow and water the guidelines of the Institutional Animal Care and Use Committee (IACUC) of Tulane University in compliance with all NIH guidelines. The ability of ASCs to form neoplastic lesions was examined *in vivo*. Briefly, the enriched nASCs or pASCs ($1 \times 10^6$; passage #<5) were primed for 72 h with either CM (1:1; *v/v*) (*n*=15), physiologic concentrations (5–10 μg/mL) of exosomes (*n*=10) derived from PC-3, C4-2B, or the normal prostate epithelial RWPE-1 cells. The cells were suspended in 50 μL of serum-free DMEM medium and an equal volume of Matrigel™ (BD Bioscience, San Jose, CA) and subsequently transplanted s.c. by a syringe fitted with a 27-gauge needle into the right and left flanks of each mouse. For negative and positive controls, mice were injected with control medium-treated nASCs, pASCs, or C4-2B into the opposite flanks. Tumor formation was monitored for up to 10 weeks. In another set of experiments, the malignant nature of pASCs nodules was validated in secondary nude mice recipients. Briefly, primary pASC tumor cells ($1 \times 10^6$; passage 3) in Matrigel™ were transplanted s.c. in nude mice and tumor formation was monitored for 4 weeks. The mice body weights and tumor sizes were measured at different time points. The tumors were excised, weighed, and stained by H&E, IHC, and immunofluorescence (IF) analysis for detection of neoplastic, vasculogenic, MET, and prostate cancer-related markers.

## Immunofluorescence

Tumors were resected from anesthetized mice after heart perfusion with PBS and parts were snap-frozen or paraffin-embedded for further analysis. The frozen sections were fixed in cold acetone/methanol (1/1 v/v) solution, washed thrice with PBS, blocked with 10% of goat serum for 1 h after washing twice with 0.2% Triton X-100 in PBS, then incubated (4°C, 12–16 h) with primary antibodies (goat anti-androgen receptor (AR), 1:100), rabbit anti-PSA (1:50), anti-rabbit α-methylacyl-CoA racemase (AMACR) (1:200), anti-rabbit anti SRD5A1 (1:100), mouse anti–cytokeratin 5/18 (CK5/18) (1:200), rabbit anti-cytokeratin 8 (CK8) (1:200), rabbit anti-Ki67 (1:200) (all from NOVUS Biologicals, Littleton, CO (http://www.novusbio.com)) as well as rabbit anti-Von Willebrand factor (1:200) (abcam, Cambridge, MA) and mouse α-smooth muscle actin (1:500 dilution) (Sigma-Aldrich, St. Louis, MO). The sections were then incubated for 1 h at room temperature in PBS/0.05% Tween-20 solution containing secondary antibodies (1:500 dilution), including donkey anti-mouse, rabbit, and goat Alex Flour 488, 594, or 647-conjugated IgGs; (Molecular Probes,

Invitrogen, Carlsbad, CA). The nuclei were stained with a 4',6-diamidino-2-phenyllindole (DAPI) mounting medium (Vectashield, Burlingame, CA). Images were acquired by confocal Leica TCS SP5 microscope/LAS AF software or Olympus IX70 inverted fluorescence microscope/MagnaFire software as previously described [4].

### Immunohistochemistry

Tissue staining was performed as previously described [20]. After blocking non-specific sites, tissues were incubated with mouse monoclonal anti-RAS (abcam, Cambridge, MA) or anti-p53 antibodies (1:50 dilution) (Biocare Medical, Concord, CA (http://www.biocare.net)) for 30 min. The antigen-antibody complex was revealed using secondary and tertiary horseradish peroxidase (HRP)-conjugated antibodies (10 min each) and visualized by beta-3,3'-diaminobenzidine (DAB) substrate-chromagen solution for 1 min. The slide sections were then counterstained by hematoxylin and bluing solution and dried up for mounting. For negative controls, the entire IHC method was performed on sections in the absence of primary antibody.

### Cytogenetic Analysis

Parental pASCs, pASC tumor cells, and C4-2B cells were cultured for 48 h (50–70% confluent). Twenty microliters of colcemid (5 μg/mL) was added to the cultured cells for 1.5 h at 37°C. Cells were then harvested in a hypotonic solution (0.75 M KCl and 0.8% Na-citrate; 1:1, *v*/*v*) and fixed in methanol/glacial acidic acid (3:1, v/v) according to standard cytogenetic techniques. The resulting metaphase cells were evaluated by Giemsa banding pattern using trypsin with Wright stain according to the standard protocols. For each sample, at least 10 metaphases were analyzed for structural rearrangements and general ploidy level. Metaphases were captured and karyotypes were prepared using the CytoVision software program (Version 3.92 Build 7) (Applied Imaging, Grand Rapids, MI (http://www.appliedimaging.com)).

### Isolation and Labeling of Exosomes

Exosomes from CM of RWPE-1, PC-3 and C4-2B cells were purified by differential centrifugation as described before with some modifications [13]. Briefly, contaminating cells were removed by centrifugation at 300 x g for 10 min, and supernatants were centrifuged at 1,200g for 20 min followed by 10,000 x g for 30 min. After filtration (0.22 μm filters), exosomes were pelleted by ultracentrifugation (Beckman ultracentrifuge, Beckman Coulter, Inc., Brea, CA) at 120,000 x g for 1 h. The pelleted exosomes were washed twice in PBS, resuspended in PBS, and stored at −80°C until used. The purity of the pelleted exosomes was verified by the expression of selective markers CD9, CD36, CD81, PDCD61P, and the epithelial cell marker epithelial cell adhesion molecule (EpCAM) by PCR analysis using a specific primer sets (Supporting information Table S2). The supernatant of the pelleted exosomes was used as a control in the PCR analysis. For cellular uptake analysis, the purified exosomes from various cells were labeled with PKH67 green fluorescent labeling kit (Sigma-Aldrich, St. Louis, MO) as reported [21]. The labeled exosomes were incubated with RWPE-1, C4-2B or pASCs in culture (5 μg per 50,000 cells) and allowed to bind for 20 min at 4°C. The cells were then washed and incubated at 37°C

and photographed after 2 h by fluorescence microscope (Nikon Instruments, Melville, NY (http://www.nikoninstruments.com)).

### Cryo-Transmission Electron Microscopy (Cryo-TEM)

The purity of isolated exosomes was corroborated by Cryo-TEM as shown previously [22]. Fresh exosome pellets from RWPE-1 and C4-2B cells were suspended in PBS and subsequently loaded on a holy carbon Cryo-TEM grid. A thin film of exosomes was established into the holes on the grid after removing excess solution by blotting filter papers. The grids were plunged into liquid ethane and transferred into Cryo-TEM (JEOL2010 model) (JEOL, Ltd., Japan (http://www.jeol.co.jp)) at the Coordinated Instrumentation Facility, Tulane University, New Orleans, USA. Images were taken in zero-loss bright field mode with an acceleration voltage of 80 kV.

### Western Blot Analysis

Immunoblot analysis was performed as previously described [23]. Briefly, cell lysates were prepared from pASCs stimulated for 72 h with CM of PC cells using RIPA lysis buffer (Santa Cruz Biotechnology, Dallas, TX). Immunoblotting was performed using primary antibodies (Novus Biologicals, Littleton, CO) against AR and PSA. Secondary antibody was applied and the signal was developed by Amersham ECL™ (GE Healthcare Bio-Sciences, Pittsburgh, PA.

### qRT-PCR Analysis and miRNA Mimics

The expression profiles of RNA in PC cells, pASCs and their transformed clones was analyzed by qRT-PCR using selective miRNAs and mRNAs primer sets (Supporting information Table S2). The miScript II kit for cDNA synthesis and SYBR Green PCR kit were purchased from Qiagen (Qiagen, Valencia, CA). The miScript Mimics were designed and used for ectopic expression of miR-125b, miR-130b or miR-155 in pASCs according a standard protocol (Qiagen, Valencia, CA). Briefly, about 70% confluent pASCs were transfected with 10 μM miR-mimics using HiPerFect transfection reagent for 24–72 h and the efficiency of transfection was evaluated by AllStars negative control siRNA AF 488 reagent at 20 μM concentration (Qiagen, Valencia, CA). Untransfected cells and cells transfected with non-targeting miR mimics were used as controls. The results were normalized to housekeeping genes (GAPDH for mRNA and RNU6 for miRNA) and expressed as fold change ± SEM from at least three independent experiments.

### Exosome miRNA Array and Proteomic Analyses

Comparative analysis of miRNA signature in exosomes derived from PC cells and RWPE-1 cells and protein contents of parental pASCs, exosome-treated pASCs and pASC tumor cells are described in Supporting Information.

### Statistical Analysis

All data are expressed as mean ± SEM. Differences between controls and experimental groups were analyzed by One Way ANOVA or Student *t*-test using GraphPad Prism 5 (GraphPad Software, Inc., La Jolla, CA). *P* values <0.05 were considered significant.

# RESULTS

## PC Cell-CM Confers Transendothelial Migration of pASCs *in vitro*

The clinicopathological characteristics of PC patients (*n*=16) whose fat tissue was used for ASCs isolation are described in Supporting information Table S1. The transduction efficiency of pASCs with pLV-eGFP construct is almost 100%. Compared with normal untransduced cells (Fig. 1A), the transduced pASCs cells retained normal morphological and growth characteristics (Figs. 1B and 1C). The purity of ASCs was verified with selective expression of mesenchymal cell surface markers CD90, CD44, CD105, and CD29 and lack of hematopoietic lineage markers CD79α, CD34, CD11b, and CD45 by FACS analysis compared with their isotype controls (Fig. 1D). The purity of pASC populations from contaminating PC cells was further confirmed by expression of the epithelial marker EpCAM by FACS analysis. Similar to nASCs, the pASCs expressed CD90, but not EpCAM, in comparison with PC-3 cells (Fig. 1E). Additionally, we verified pASCs are MSCs by examining their ability to exhibit adipogenic, osteogenic and chondrogenic differentiation *in vitro* (Supporting information Fig. S1). The transendothelial cell migration of pLV-eGFP-transduced pASCs derived from PC patients was measured in a trans-well culture system. Although no difference was observed in the migration ability of nASCs towards the CM of PC or normal RWPE-1 cells, four pASC isolates had higher TEM towards CM of LNCaP cells (Fig. 1F) and C4-2B cells (Fig. 1G) in comparison with CM of RWPE-1 cells, suggesting that pASCs have higher tumor tropism than nASCs.

The RT2 Profiler custom PCR array analysis revealed selective expression of cell surface markers in the migrating pASCs compared with non-migratory cell populations. These included cell adhesion molecules (cadherin1, type 1; Cadherin 6, type 2; and integrin-α7), extracellular matrix degrading proteins (stromelysin 2 and 3 subtypes), growth factors (hepatocyte growth factor and insulin-like growth factor-1), chemokines (chemokine ligend 7) and activation receptors (tumor necrosis factor receptor-10 and fibroblast growth factor receptor-4) (Supporting information Fig. S2).

## pASCs Primed with PC Cell-CM Form Prostate-Like Neoplastic Lesions and Undergo MET *in vivo*

Because of their plasticity and high tumor homing potential, we sought to examine whether pASCs exposed to CM of PC cells will transdifferentiate and form tumors *in vivo*. The tumor-tropic pASCs or nASCs were exposed to CM of C4-2B, PC-3, or RWPE-1 cells for 72 h *in vitro* and then transplanted s.c. into the opposite flanks of athymic nude mice. Other transplanted controls included RWPE-1 cells and control medium-treated pASCs. Subcutaneous nodular formation developed within 8 to 10 weeks by pASCs treated PC cell-derived CM (left flank), but not by CM of RWPE-1 cells (right flank) in 11 out of 15 mice (Fig. 2A). Consistent with C4-2B tumors (left panel), the pASC nodules (right panel) revealed neoplastic histopathological features suggestive of PC mimicry marked with large nucleoli and capillary formation (Fig. 2B) and expression of AR and PSA, as evidenced by immunoblotting (Fig. 2C) and IHC (Fig. 2D) analyses. Marked expression of PC related markers, including CK8 (Fig. 2E) and CK5/18 (Fig. 2F) and the PC-specific marker, AMACR, (Fig. 3A) was also discernible in pASC tumors, and further corroborate these

findings. Importantly, large aggressive tumors developed within 4 weeks in secondary recipients following serial transplantation of pASC tumor cells (Fig. 2G), further attesting to the neoplastic nature of these cells. The poorly differentiated pASC tumors are marked with large nucleoli and neovasculature (right panels), similar to PC cell (PC-3 or C4-2B) tumors from which they were originally derived (left panels) (Fig. 2H). Noteworthy, not only the morphology of pASC tumor cells changed from their spindle-like (Fig. 2I) to flattened rounded cells (Fig. 2J), but also their *in vitro* proliferative capacities were significantly higher than their parental pASC cells (Fig. 2K). Based on flow cytometry results, only 8.7% and 5.7% of cell population expressed pan-cytokeratin (pan-$CK^+$) and $CD44^+$, respectively, whereas the majority (84.3%) pASC tumor cells had a $CD44^+$/pan-$CK^+$ expression phenotype (Fig. 2L). This was in stark contrast to the phenotype of the parental pASCs, primarily $CD44^+$/pan-$CK^-$, or the C4-2B cells ($CD44^-$/pan-$CK^+$), suggesting acquisition of MET by pASC tumor cells. The MET of pASC tumor cells (passage 3) was further corroborated by intense pan-CK expression (red fluorescence, middle panel) in comparison to C4-2B cells (upper panel) and the parental pASCs (lower panel) (Fig. 2M).

The neoplastic nature of the pASC-derived nodules was further validated by the expression of tumorigenic markers, Ki67, p53, and Ras reminiscent of the molecular features of C4-2B tumors (Figs. 3B–D) and the vaculogenic markers, Willebrand Factor and α-smooth muscle actin, selective markers for blood vessel endothelium (Fig. 3E). Similar to PC cells (Supporting information, Fig. S3C), karyotype analysis demonstrates an array of cytogenetic aberrations suggestive of genetic instability (tetraploidy, chromosomal abnormalities, polymorphism, and extended p arm) in pASC tumor cells (Supporting information Fig. S3B, Table S3). This was in stark contrast to the normal karyotype of the isogenic parental pASCs, further attesting to the neoplastic genotypic alteration of pASCs (Supporting information, Fig. S3A).

### PC Cell-Derived Exosomes trigger Neoplastic Transformation and MET by pASCs *in vivo*

As a component of PC cell CM, we examined the functional significance of exosomes in the genesis of neoplastic lesions and MET by pASC cells. Exosomes were isolated from PC and RWPE-1 cells and their integrities and purities were verified by Cryo-TEM (Fig. 4A) and selective expression of exosome-related markers (Fig. 4B). The PKH67-stained exosomes were rapidly and efficiently internalized within 2 h with uniform cytoplasmic distribution in >95% of pASCs *in vitro* (Fig. 4C). Compared with RWPE-1 cells or control media, treatment with physiologic concentrations of C4-2B–derived exosomes (5 μg/mL) for 24 h caused upregulation of AR and PSA transcripts in pASCs (Fig. 4D). Next, we examined whether nASCs or pASCs treated with PC-3, C4-2B or RWPE-1 cell-derived exosomes, or CM for 72 h form tumors *in vivo*. Like cells treated with PC cell CM (left flank), the PC-3 and C4-2B cell associated exosomes (right flank) enabled tumor formation by the same pASC isolates in 80% ($n$=10) of mice studied in 10 weeks (Fig. 4E). However, neither PC-3 nor C4-2B associated exosomes were able to generate tumors in nASC injected mice. Similarly, RWPE-1-derived exosomes were not sufficient to generate tumors by pASCs. The histopathological features of tumors generated by exosomes were recapitulative of tumors developed by PC cells and PC cells CM (Fig. 4F). In comparison to parental pASCs and C4-2B cells, the pattern of expression profiles of CD44 and pan-CK in exosome derived

pASC tumor cells was analogous to those exhibited by CM-induced pASC tumor cells (Fig. 4G), suggesting that MET is primarily driven by PC cell-associated exosomes.

## Neoplastic Reprogramming is Attributed to PC Cell-Derived Exosome Trafficking of Oncogenic Factors Into pASCs

Exosome differential miRNA array analysis unraveled selective oncogenic miRNA signatures (miR-125b, miR-130b, and miR-155) potentially involved in induction of neoplastic transformation and MET in pASCs by PC cell associated exosomes (Supporting information, Fig. S4). Similar to miRNA-expression profiles in C4-2B and pASC tumor cells, the C4-2B cell-derived exosomes were found to harbor higher endogenous levels (3-fold) of miR-125b, miR-130b compared with RWPE-1-derived exosomes or parental pASCs (Figs. 5A and 5B, Supporting information, Fig. S4). Compared with isogenic parental cells, the recipient pASCs treated for up to 72 h with PC cell derived exosomes had 11-fold and 2.5–fold for 125b and 130b, respectively, which paralleled their expression profile in their isogenic pASC-derived tumor cells (Fig. 5C and Fig. 5D). The exosome transfer of the oncomiRNAs was coupled with upregulation of H-*ras* and K-*ras* and down-regulation of the tumor suppressors, Lats2 and PDCD4 in exosome-treated pASCs and their derived tumor cells as opposed to RWPE-1-derived exosomes or isogenic parental pASCs (Figs. 5E–H).

The microRNA Target Prediction and Functional Study Databases (http://mirdb.org/miRDB) and target scans (http://www.targetscan.org) identified a number of known and predicted miRNAs implicated in transcriptional upregulation of AR, PSA, AMACR, CK5, angiogenesis, and MET-related genes in the PC-derived exosomes miRNA signature (Supporting information, Table S4). The LC/MS/MS analysis revealed selective protein signature in C4-2B cell-derived exosomes in comparison with RWPE-1-derived exosomes (Fig. 5I). The signature encompasses a wide array of proteins implicated in oncogenesis, MET, stress response proteins, signal transduction, transcription factors, cell growth and migration, mRNA processing and cell transport mechanisms and survival (Supporting information, Table S5). Importantly, most of the oncogenic proteins, including RAB1a, RAB1b, and RAB11a which are regulators of membrane trafficking and exosome formation, were effectively transferred to the recipient pASCs by PC cell-derived exosomes and were equally expressed in the pASC tumor cells (Figs. 5J and 5K, Supporting information Table S6).

Next we examined by miR-mimics strategy the functional significance of oncomiRNAs in modulating transcription of oncogenic factors and tumor suppressors in pASCs. As shown in Fig. 6A, upregulation of oncomiRNAs miR-125b, miR-130b, and miR-155 peaked at 24 hrs in pASCs compared with mock-transfected cells. The expressed oncomiRNAs caused upregulation of H-*ras* and K-*ras* (Figs. 6B and 6C) and down-regulation of the tumor suppressors, Lats2 and PDCD4 (Figs. 6D and 6E), suggesting that their dysregulation may be attributed to trafficking and expression of these oncomiRNAs by C4-2B cell-derived exosomes into the recipient stem cells. These finding were corroborated by similar expression pattern of miR-125b and miR-155 ($P<0.001$) (Fig. 7A), the tumor suppressor PDCD4 (Fig. 7B) ($P<0.05$), H-*ras* and K-*ras* ($P<0.05$) (Figs. 7C and 7D) in microdissected

human prostate tumor cells (*n*=18) in comparison to adjacent normal glands (Supporting information, Table S7).

## DISCUSSION

Mesenchymal stem cells are multipotent, self-renewing cells that are amenable to differentiation into specialized cells [24] encompassing osteoblasts, chondrocytes, myocytes, and adipocytes [25]. Although tissue specific fates of MSCs under defined conditions are well established, their ability to transform into tumor cells upon exposure to cancer cell-derived factors has not been elucidated. We report a previously uncharacterized mechanism related to *in vivo* genesis of neoplastic lesions by PC cell-CM primed pASCs that were grossly and histologically comparable with those developed by PC cells. The malignant nature of pASC lesions was validated by tumor development in secondary recipients, cytogenetic aberrations, and by the expression of neoplastic, vasculogenic, and MET markers. Conversely, the untreated pASCs had normal cytogenetic profiles and did not form tumors *in vivo* when transplanted individually or treated with CM or exosomes of normal prostate cells. Additionally, neither human primary prostate epithelial cells (hPrEC) nor RWPE-1 cells treated with PC-derived exosomes formed tumors *in vivo* (Abdel-Mageed's unpublished observation). This suggests that the neoplastic transformation of tumor-tropic pASCs may be triggered by unique intrinsic and cell surface properties as a consequence of their long-term exposure to tumor-derived oncogenic factors in PC patients. Altogether, our data suggest that, when triggered by circulating tumor cell derived factors, tumor-tropic ASCs undergo tumor mimicry and may contribute to disease progression in cancer patients by increasing cancer clonal expansion at localized and metastatic sites. Our results also indicate that allogeneic adult ASCs procured from donors with otherwise undetected malignancies may make them non-amenable for therapeutic transplantations, thus underscoring ASC monitoring in clinical settings. Whether such effects extend to other tumor-tropic MSCs remains to be elucidated.

Our mechanistic studies identified exosomes as the primary component of PC cell derived factors involved in enabling neoplastic transformation and MET by pASCs. Exposure of pASCs to physiologic concentrations of PC cell-derived exosomes was sufficient to reproduce malignant lesions conferred by PC cell CM, with a predominant MET phenotype. In cancer patients, the release of tumor associated exosomes in biofluids correlates with disease progression, increasing several folds compared with healthy subjects [16, 26, 27]. Thus our study supports a novel role for circulating tumor-derived exosomes in promoting tumor and metastatic outgrowth through induction of neoplastic transformation and MET by pASCs in cancer patients. Therefore, our finding brings novel insights to the current concept that disseminated or circulating tumor cells are the primary and sole culprits of metastatic disease [28].

Our cytodifferentiation studies showed that pASC tumor cells express markers reminiscent of MET, with the majority of cells maintaining both epithelial and mesenchymal phenotypes. A strong association between MET and metastatic tumor development [29], including PC [30], has been established. This association suggests that the clonal expansion of metastatic tumors in cancer patients may be related to MET by the tumor recruited

pASCs. Conversely, the epithelial-to-mesenchymal transition (EMT) at the tumor-stroma interface has been implicated in enhanced invasive behavior of cancer cells of epithelial origin [31]. Our results thus argue that EMT and MET in the metastatic niche arises solely from metastatic tumor cells in cancer patients. Additionally, our findings of pASC tumor mimicry may also narrow the significant gap in the current knowledge linking obesity to PC progression.

In the tumor microenvironment, exosomes emanating from cancer cells may alter the phenotype and biological behavior of normal or indolent cells through intercellular trafficking of functionally translated oncogenic materials, including oncogenic DNA, activated oncoproteins and their transcripts, and oncogenic and regulatory microRNA [32, 33]. As equally evidenced in human microdissected prostate tumors, our study shows that exosomes derived from metastatic PC, but not RWPE-1, cells not only harbor, but also transfer H-*ras* and K-*ras* transcripts to pASCs. Mutation of the three Ras proto-oncogenes (H-, K-, and N-*ras*) is frequently detected in many human tumors, including PC [34]. Indeed, PC-3 cells and LNCaP, the isogenic parental cells of C4-2B cells, have a K-*ras* mutation [35], and aberrations and activation of Ras/Raf pathways are among the most frequently occurring genetic changes in PC. This result accounts for more than 40% of prostate primary tumors and 90% of metastatic PC [36]. Although cellular Ras gene activity is crucial to virally induced neoplastic transformation [37], both mutant K-*ras* and H-*ras* have been shown to be important genetic elements in the tumorigenic transformation of normal human epithelial and fibroblast cells [38, 39]. Represented by at least 30 different Ras oncogene superfamily, Rab proteins facilitate vesicle identification and/or fusion with target cells [40], suggesting their potential role in tumorigenesis. In the present study, we identified transfer to and expression in pASCs by PC-cell derived exosomes of Rab1a and Rab1b and the endosomal recycling of Rab GTPase Rab11a, implicated in various human tumors [41–43]. Based on their oncogenic properties, our findings indicate that mutant K-*ras* and H-*ras* and/or Rab proteins in tumor-derived exosome cargo may contribute to PC progression through induction of tumorigenic transformation of pASCs.

MicroRNAs have been shown to play a direct role in many cancers as tumor suppressors or oncogenes by targeting mRNA of tumor suppressor genes, including PC [44]. Our analysis revealed a distinctive dysregulated oncomiRNA repertoire and a subset involved in transcriptional upregulation of AR, PSA, angiogenesis, and epithelial markers in PC cell derived exosomes. Overexpression of miR-130b caused tumorigenesis by targeting the tumor suppressor RUNX3 [45], or TP53INP1 [46]. The miR-125b initiated tumors [47] through primary or secondary events in a variety of cancers, including PC [48]. As an oncogene, miR-155 regulated cell survival in breast cancer [49] and B-cell lymphoma developed in miR-155 transgenic mice [50]. Thus the neoplastic transformation of pASCs may have been a consequence of the transport by PC-derived exosomes and functional activation of these oncomiRNAs, along with Ras related oncogenic factors

Tumor-derived exosomes may also inhibit tumor suppressors to promote tumorigenesis. Our miRNA mimiced expression of miR-125b and miR-130b caused down-regulation of tumor suppressors Lats2 and PDCD4 in pASCs treated with PC cell-derived exosomes. Lats2 and PDCD4 have been shown to inhibit tumor formation [51, 52]. Although p53 is a direct target

for miR-125b [53], miR-155 and miR-130b induce their oncogenic activities primarily through targeted degradation of p53-induced nuclear protein 1 (TP53INP1) [54]. Thus we speculate that the dysregulated expression of oncomiRNA repertoire caused neoplastic transformation of pASCs through dysregulation of transcriptional networks of tumor suppressor genes Lats2 and PDCD4.

## CONCLUSION

Our proposed model implicates that transport and expression of functional oncogenic factors in pASCs via PC cell-derived exosomes confer genetic instability, MET, and oncogenic transformation of tumors in recruited pASCs (Fig.7E). The model demonstrates a novel role for a potential tumor-derived exosome-pASC axis in neoplastic transformation, phenotypic transition in tumor's mesenchymal-to-epithelial states, and disease progression in PC patients as well as in other types of cancers. Based on their trafficking ability, plasticity, and tumor-homing potential, our findings propose a new phenomenon by which tumor cells may exploit tumor recruited adult ASCs, whether tissue resident or circulating, to enhance their clonal expansion at primary and metastatic sites through neoplastic mimicry which consequently increases the tumor burden in PC patients. Thus our findings are invaluable for defining new insights into the molecular perturbations that drive the transformation of adult stem cells and further suggest that therapeutic targeting of tumor-derived exosomes or their "cargo" may have significant diagnostic, prognostic and therapeutic implications in the clinical management of cancer patients with localized and advanced disease.

## Supplementary Material

Refer to Web version on PubMed Central for supplementary material.

## Acknowledgments

This work was partially supported by grants from the National Cancer Institute and National Center for Advancing Translational Sciences (NCATS), National Institutes of Health (5U01CA149204-03; CA149204-01A1; A.B.A), American Cancer Society (RSGT-09-248-01-CCE; A.B.A), and Department of Defense grants (PC102056; A.B.A.; and PC080811, D.M.). We would like to thank Mrs. Nancy Busija (MA, CCC-SLP) for editing the manuscript.

## REFERENCES

1. Huggins C, Hodges CV. Studies on prostatic cancer. I. The effect of castration, of estrogen and androgen injection on serum phosphatases in metastatic carcinoma of the prostate. CA Cancer J Clin. 1972; 22:232–240. [PubMed: 4625049]
2. Keto CJ, Aronson WJ, Terris MK, et al. Obesity is associated with castration-resistant disease and metastasis in men treated with androgen deprivation therapy after radical prostatectomy: results from the SEARCH database. BJU Int. 2012; 110:492–498. [PubMed: 22094083]
3. Planat-Benard V, Silvestre JS, Cousin B, et al. Plasticity of human adipose lineage cells toward endothelial cells: physiological and therapeutic perspectives. Circulation. 2004; 109:656–663. [PubMed: 14734516]
4. Ma L, Yang Y, Sikka SC, et al. Adipose tissue-derived stem cell-seeded small intestinal submucosa for tunica albuginea grafting and reconstruction. Proc Natl Acad Sci USA. 2012; 109:2090–2095. [PubMed: 22308363]

5. Klopp AH, Gupta A, Spaeth E, Andreeff M, Marini F. Concise review: Dissecting a discrepancy in the literature: do mesenchymal stem cells support or suppress tumor growth? Stem Cells. 2011; 29:11–19. [PubMed: 21280155]
6. Huelsken J. Tissue-specific stem cells: friend or foe? Cell. Res. 2009; 19:279–281. [PubMed: 19252511]
7. Bellows CF, Zhang Y, Chen J, Frazier ML, Kolonin MG. Circulation of progenitor cells in obese and lean colorectal cancer patients. Cancer Epidemiol. Biomarkers Prev. 2011; 20:2461–2468. [PubMed: 21930958]
8. Brennen WN, Chen S, Denmeade SR, Isaacs JT. Quantification of mesenchymal stem cells (MSCs) at sites of human prostate cancer. Oncotarget. 2013; 4:106–117. [PubMed: 23362217]
9. Lee Y, El Andaloussi S, Wood MJ. Exosomes and microvesicles: extracellular vesicles for genetic information transfer and gene therapy. Hum Mol Genet. 2012; 15:R125–R134. [PubMed: 22872698]
10. Thery C, Zitvogel L, Amigorena S. Exosomes: composition, biogenesis and function. Nat Rev Immuno. 2002; 2:569–579.
11. Lakkaraju A. Rodriguez-Boulan E. Itinerant exosomes: emerging roles in cell and tissue polarity. Trends Cell Biol. 2008; 18:199–209. [PubMed: 18396047]
12. Hugel B, Martinez MC, Kunzelmann C, Freyssinet JM. Membrane microparticles: two sides of the coin. Physiology (Bethesda). 2005; 20:22–27. [PubMed: 15653836]
13. Skog J, Wurdinger T, van Rijn S, et al. Glioblastoma microvesicles transport RNA and proteins that promote tumour growth and provide diagnostic biomarkers. Nat Cell Biol. 2008; 10:1470–1476. [PubMed: 19011622]
14. Peinado H, Aleckovic M, Lavotshkin S, et al. Melanoma exosomes educate bone marrow progenitor cells toward a pro-metastatic phenotype through MET. Nat Med. 2012; 18:883–891. [PubMed: 22635005]
15. Bartel DP. MicroRNAs: target recognition and regulatory functions. Cell. 2009; 136:215–233. [PubMed: 19167326]
16. Rabinowits G, Gercel-Taylor C, Day JM, Taylor DD, Kloecker GH. Exosomal microRNA: a diagnostic marker for lung cancer. Clin Lung Cancer. 2009; 10:42–46. [PubMed: 19289371]
17. Eis PS, Tam W, Sun L, Chadburn A, et al. Accumulation of miR-155 and BIC RNA in human B cell lymphomas. Proc Natl Acad Sci USA. 2005; 102:3627–3632. [PubMed: 15738415]
18. Johnson SM, Grosshans H, Shingara J, et al. RAS is regulated by the let-7 microRNA family. Cell. 2005; 120:635–647. [PubMed: 15766527]
19. Graham TR, Agrawal KC, Abdel-Mageed AB. Independent and cooperative roles of tumor necrosis factor-alpha, nuclear factor-kappaB, and bone morphogenetic protein-2 in regulation of metastasis and osteomimicry of prostate cancer cells and differentiation and mineralization of MC3T3-E1 osteoblast-like cells. Cancer Sci. 2009; 101:103–111. [PubMed: 19811499]
20. Abd Elmageed ZY, Moroz K, Srivastav SK, et al. High circulating estrogens and selective expression of ERβ in prostate tumors of Americans: implications for racial disparity of prostate cancer. Carcinogenesis. Jun 19.2013 [Epub ahead of print].
21. Liu C, Yu S, Zinn K, et al. Murine mammary carcinoma exosomes promote tumor growth by suppression of NK cell function. J Immunol. 2006; 176:1375–1385. [PubMed: 16424164]
22. Dubochet J, Adrian M, Chang JJ, et al. Cryo-electron microscopy of vitrified specimens. Q Rev Biophys. 1988; 21:129–228. [PubMed: 3043536]
23. Abdel-Mageed AB, Agrawal KC. Activation of nuclear factor kappaB: potential role in metallothionein-mediated mitogenic response. Cancer Res. 1998; 58:2335–2338. [PubMed: 9622069]
24. Segers VF, Lee RT. Stem-cell therapy for cardiac disease. Nature. 2008; 451:937–942. [PubMed: 18288183]
25. Collas P. Programming differentiation potential in mesenchymal stem cells. Epigenetics. 2010; 5:476–482. [PubMed: 20574163]
26. Taylor DD, Lyons KS, Gercel-Taylor C. Shed membrane fragment-associated markers for endometrial and ovarian cancers. Gynecol. Oncol. 2002; 84:443–448. [PubMed: 11855885]

27. Andre F, Schartz NE, Movassagh M, et al. Malignant effusions and immunogenic tumour-derived exosomes. Lancet. 2002; 360:295–305. [PubMed: 12147373]
28. Tsouma A, Aggeli C, Pissimissis N, Lembessis P, Zografos GN, Koutsilieris M. Circulating tumor cells in colorectal cancer: detection methods and clinical significance. Anticancer Res. 2008; 28:3945–3960. [PubMed: 19192655]
29. Yao D, Dai C, Peng S. Mechanism of the mesenchymal-epithelial transition and its relationship with metastatic tumor formation. Mol. Cancer Res. 201; 9:1608–1620. [PubMed: 21840933]
30. Oltean S, Sorg BS, Albrecht T, et al. Alternative inclusion of fibroblast growth factor receptor 2 exon IIIc in Dunning prostate tumors reveals unexpected epithelial mesenchymal plasticity. Proc Natl Acad Sci USA. 2006; 103:14116–14123. [PubMed: 16963563]
31. Kang Y, Massague J. Epithelial-mesenchymal transitions: twist in development and metastasis. Cell. 2004; 118:277–279. [PubMed: 15294153]
32. RakJ, GuhaA. Extracellular vesicles vehicles that spread cancer genes. Bioessays. 2012; 34:489–497. [PubMed: 22442051]
33. Zomer A, Vendrig T, Hopmans ES, van Eijndhoven M, Middeldorp JM, Pegtel DM. Exosomes: fit to deliversmall RNA. Commun. Integ Biol. 2010; 3:447–450.
34. Shen Y, Lu Y, Yin X, Zhu G, Zhu J. KRAS and BRAF mutations in prostate carcinomas of Chinese patients. Cancer Genet Cytogene. 2010; 198:35–39.
35. Rajesh D, SchellK, Verma AK. Ras mutation, irrespective of cell type and p53 status, determines a cell's destiny to undergo apoptosis by okadaic acid, an inhibitor of protein phosphatase 1 and 2A. Mol Pharmacol. 1999; 56:515–525. [PubMed: 10462539]
36. Taylor BS, Schultz N, Hieronymus H, et al. Integrative genomic profiling of human prostate cancer. Cancer Cell. 2010; 18:11–22. [PubMed: 20579941]
37. Raptis L, Marcellus R, Corbley MJ, et al. Cellular ras gene activity is required for full neoplastic transformation by polyomavirus. J Virol. 1991; 65:5203–5210. [PubMed: 1654439]
38. Hahn WC, Counter CM, Lundberg AS, Beijersbergen RL, Brooks MW, Weinberg RA. Creation of human tumour cells with defined genetic elements. Nature. 1999; 400:464–468. [PubMed: 10440377]
39. Parda DS, Thraves PJ, Kuettel MR, et al. Neoplastic transformation of a human prostate epithelial cell line by the v-Ki-ras oncogene. Prostate. 1993; 23:91–98. [PubMed: 8378190]
40. Novick P, Brennwald P. Friends and family: the role of the Rab GTPases in vesicular traffic. Cell. 1993; 75:597–601. [PubMed: 8242735]
41. Shimada K, Uzawa K, Kato M, et al. Aberrant expression of RAB1A in human tongue cancer. Br. J. Cancer. 2005; 92:1915–1921. [PubMed: 15870709]
42. He H, Dai F, Yu L, et al. Identification and characterization of nine novel human small GTPases showing variable expressions in liver cancer tissues. Gene Expr. 2002; 10:231–242. [PubMed: 12450215]
43. Palmieri D, Bouadis A, Ronchetti R, Merino MJ, Steeg PS. Rab11a differentially modulates epidermal growth factor-induced proliferation and motility in immortal breast cells. Breast Cancer Res Treat. 2006; 100:127–137. [PubMed: 16791477]
44. Sevli S, Uzumcu A, Solak M, Ittmann M, Ozen M. The function of microRNAs, small but potent molecules, in human prostate cancer. Prostate Cancer Prostatic Dis. 2010; 13:208–217. [PubMed: 20585343]
45. Lai KW, Koh KX, Loh M, et al. MicroRNA-130b regulates the tumour suppressor RUNX3 in gastric cancer. Eur J Cancer. 2010; 46:1456–1463. [PubMed: 20176475]
46. Ma S, Tang KH, Chan YP, et al. miR-130b Promotes CD133(+) liver tumor-initiating cell growth and self-renewal via tumor protein 53-induced nuclear protein 1. Cell Stem Cell. 2010; 7:694–707. [PubMed: 21112564]
47. Bousquet M, Harris MH, Zhou B, Lodish HF. MicroRNA miR-125b causes leukemia. Proc Natl Acad Sci U S A. 2010; 107:21558–21563. [PubMed: 21118985]
48. Shi XB, Xue L, Ma AH, Tepper CG, Kung HJ, White RW. miR-125b promotes growth of prostate cancer xenograft tumor through targeting pro-apoptotic genes. Prostate. 2011; 71:538–549. [PubMed: 20886540]

49. Kong W, He L, Coppola M, et al. MicroRNA-155 regulates cell survival, growth, and chemosensitivity by targeting FOXO3a in breast cancer. J.Biol Chem. 2010; 285:17869–17879. [PubMed: 20371610]
50. Costinean S, Zanesi N, Pekarsky Y, et al. Pre-B cell proliferation and lymphoblastic leukemia/high-grade lymphoma in E(mu)-miR155 transgenic mice. Proc Natl Acad Sci U S A. 2006; 103:7024–7029. [PubMed: 16641092]
51. Li Y, Pei J, Xia H, Ke H, Wang H, Tao W. Lats2, a putative tumor suppressor, inhibits G1/S transition. Oncogene. 2003; 22:4398–4405. [PubMed: 12853976]
52. Schmid T, Jansen AP, Baker AR, Hegamyer G, Hagan JP, Colburn NH. Translation inhibitor Pdcd4 is targeted for degradation during tumor promotion. Cancer Res. 2008; 68:1254–1260. [PubMed: 18296647]
53. Le MT, Teh C, Shyh-Chang N, et al. MicroRNA-125b is a novel negative regulator of p53. Genes Dev. 2009; 23:862–876. [PubMed: 19293287]
54. Gironella M, Seux M, Xie MJ, et al. Tumor protein 53-induced nuclear protein 1 expression is repressed by miR-155, and its restoration inhibits pancreatic tumor development. Proc Natl Acad Sci U S A. 2007; 104:16170–16175. [PubMed: 17911264]

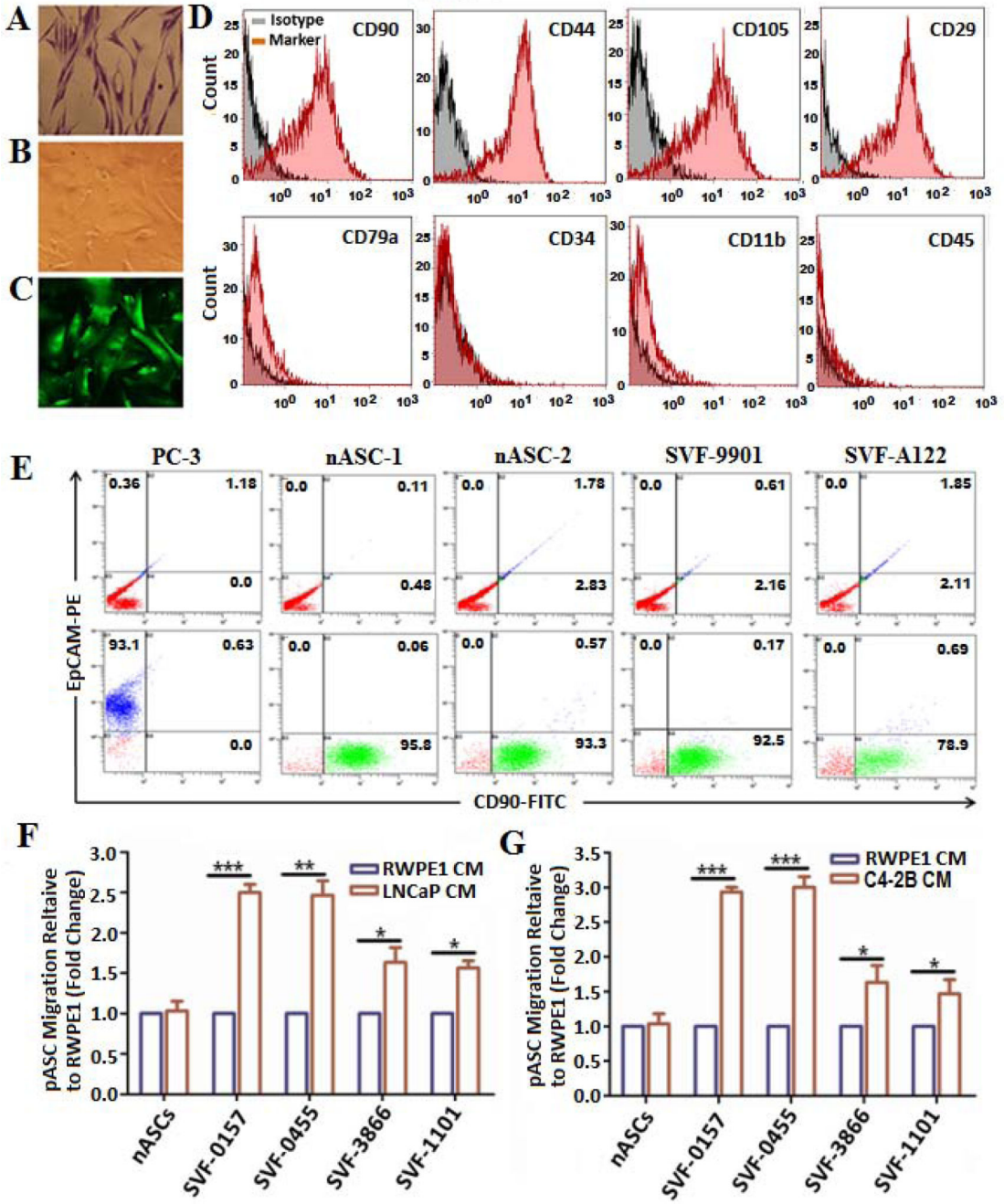


**Figure 1. Isolation, characterization and transendothelial migration of patient-derived ASCs towards PC cell-CM *in vitro***

Representative photomicrographs of methylene blue stained patient-derived ASCs (pASCs) depicting retention of fibroblast-like phenotype (**A**) in comparison to parental cells stably transduced with a lentivirus construct expressing green fluorescent protein (pLV-eGFP) under bright field (**B**) and fluorescence microscope (**C**) (*40x*). (**D**) Purity of isolated pASCs was verified by FACS analysis of mesenchymal surface expression markers CD90, CD44, CD105, and CD29 (upper panel) and of hematopoietic lineage markers CD79α, CD34,

CD11b, and CD45 (lower panel) compared with their isotype controls. (**E**) Representative FACS analysis of CD90-FITC and the epithelial marker EpCAM-PE to determine purity of pASCs (designated SVF-9901 and SVF-A122) against normal ASCs (nASC-1 and nASC-2) and PC-3 cells (lower panel) versus control isotype (upper panel). (**F, G**) Transendothelial migration of pLV-eGFP-labeled nASCs and pASCs (SVF-0157, SVF-0455, SVF-3866, and SVF-1101) through a confluent layer of hBMEC-1/basement membrane barrier towards CM of LNCaP, C4-2B, or RWPE-1 cells in the lower chambers. The pASCs migration was monitored in quadruplicates after 24 h by a fluorescence plate reader, normalized to RWPE-1 cells and expressed as a fold change in fluorescence intensity relative to nASCs by three independent experiments. * $p<0.05$, ** $p<0.01$ and *** $p<0.001$.

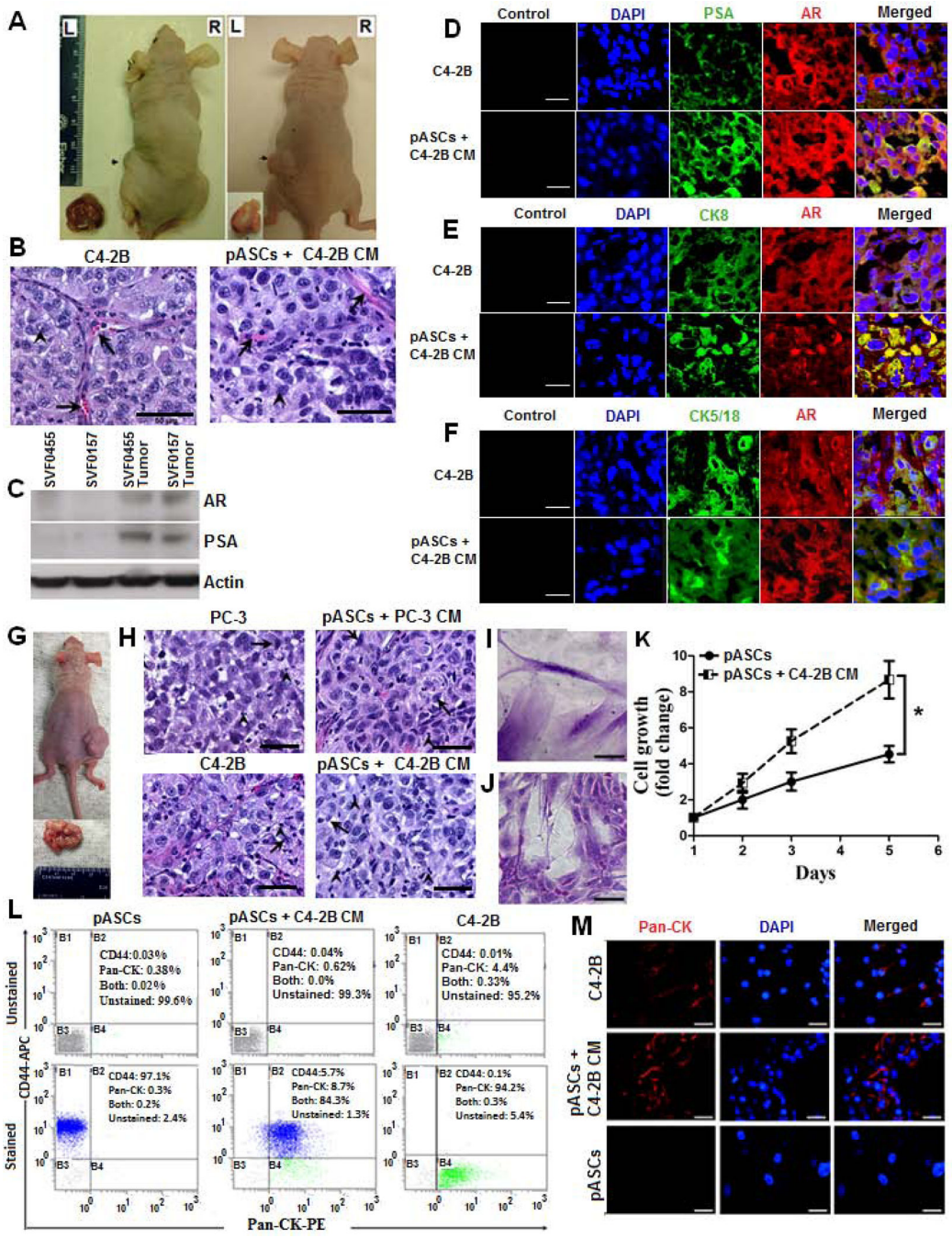


**Figure 2. pASCs primed with C4-2B cell-derived conditioned medium develop prostate neoplastic lesions and undergo MET *in vivo***

(**A**) Representative nude mice demonstrating tumor formation in the left flanks within 8 to 10 weeks by pASCs (SVF-0455 and SVF-0157) primed with conditioned medium (CM) of C4-2B cells versus no tumor formation in the right flanks by the same pASCs when primed with CM of RWPE-1 cells. Dissected tumors are shown in bottom insets. Scale bar, 50 μm. (**B**) Photomicrograph of Hematoxylin/Eosin (H&E) stained tumor sections (200x) of C4-2B cells (left panel) and pASCs treated with C4-2B cell-CM (right panel) are shown. Prominent

nucleoli (*arrowhead*) and thin capillaries (*arrow*) are present. (**C**) Immunoblot analysis of PC epithelial markers (AR and PSA) in parental pASCs (SVF0455 and SVF0157) and in their tumor-derived sublines. (**D-F**) Confocal microscopic analysis depicting expression of PC markers of AR and PSA, CK8, and CK5/18 in tumor xenografts derived from C4-2B and C4-2B CM-treated pASCs. AR (red) and PSA, CK8 and CK5/18 (green) are shown as individual channels and as merged channels with AR. Scale bar, 25 μm. (**G**) Serial transplantation of cells isolated from primary pASC tumors (SVF-0455) developed larger and more aggressive tumors within 4 weeks in secondary recipients. Tumor size is shown in bottom insets. (**H**) H&E stained tumor sections of PC-3 or C4-2B tumors (left panels) and their respective CM- generated pASC tumors in secondary recipients (right panels) showing poorly differentiated carcinomas with prominent nucleoli. Focal gland formation was evident by occasional clusters of cells with signet-ring morphology (*arrows*). Scattered inflammatory cells (arrowhead) and thin capillaries were also present. Scale bar, 50 μm. (**I, J**) Bright field photomicrographs show spindle-shaped morphology of methylene blue stained parental pASCs and their isogenic tumor-derived pASCs (small flat-shaped), respectively. (**K**) Growth rate kinetics of parental and pASC tumor cells as measured by WST-8 colorimetric assay. (**L**) Single cell suspension (*passage 3*) of pASC tumors, generated by C4-2B cell CM were double-stained for CD44-APC and Pan-CK-PE and percent expression of each marker was analyzed by flow cytometry in four separate quadrants (B1-B4). Naïve pASCs and C4-2B cells were used as controls. The percentage of pASC tumor cells expressing CD44 (B1), pan-CK (B4), both markers (B2), and unstained population (B3) is shown (lower panel) relative to control unstained cells (upper panel). (**M**) Cells isolated from primary pASC tumors (SVF-B123) and tumor xenografts generated by C4-2B CM (middle panel) were expanded in culture (passage 3) and subsequently stained for Pan-CK expression (red) by immunofluorescence analysis. Parental pASCs (bottom panel) and C4-2B (upper panel) were used as negative and positive controls, respectively. Nuclei were stained with DAPI (blue). Scale bars denote 50 μm. Cell Culture data is expressed as fold change ± SEM relative to day 1. * denotes significance at $p<0.05$.

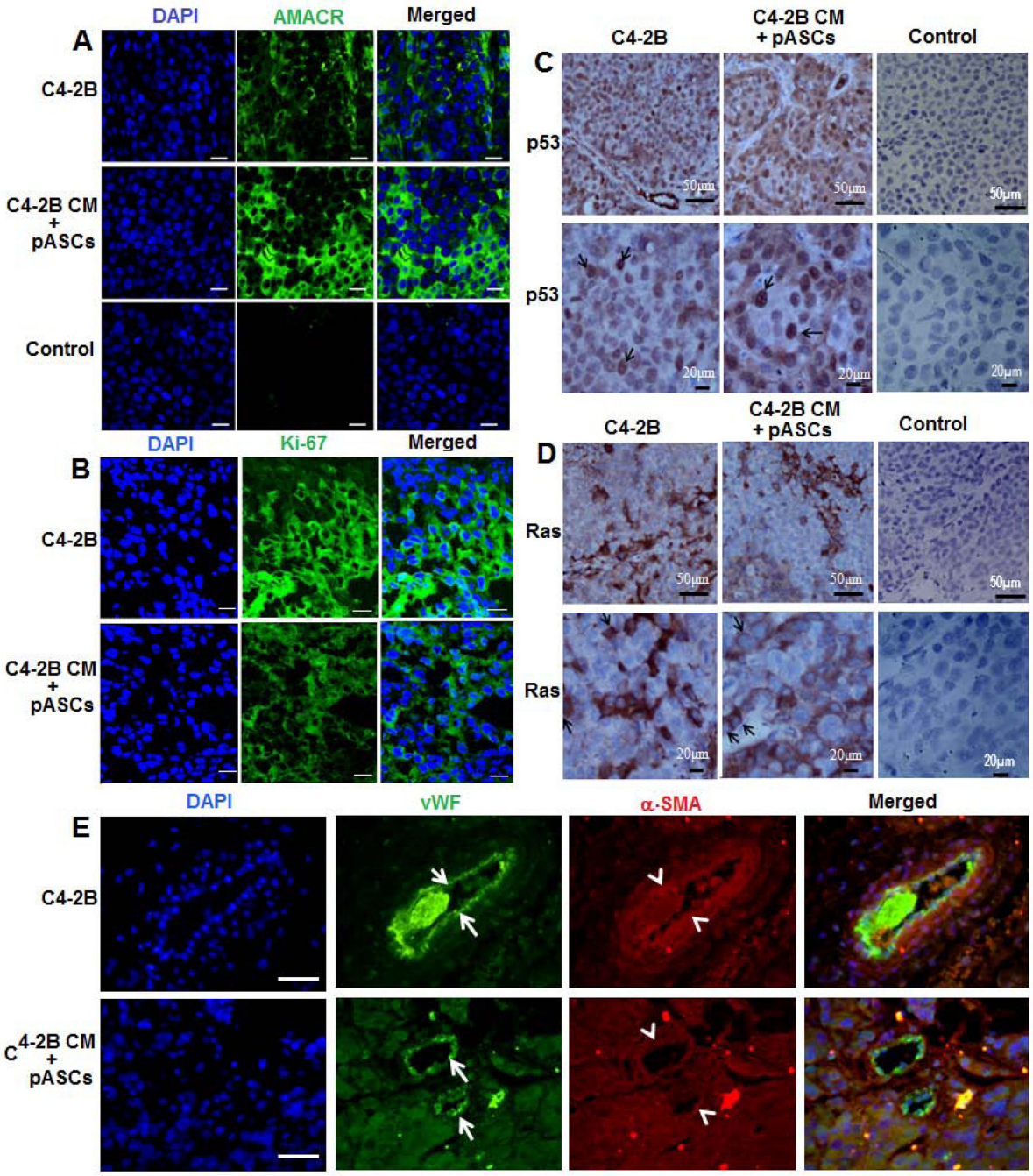


**Figure 3. Expression of neoplastic, vasculogenic, and PC-specific markers in pASC tumor xenografts**

(**A**): Confocal microscopic analysis of AMACR, a PC specific marker, in immunofluorescent stained tumor sections of C4-2B (upper panels) versus pASCs treated with CM of C4-2B cells (middle panels). Intense cytoplasmic immunostaining of AMACR (*green*) is observed in both xenografts. Lower panels depict control sections in absence of primary antibody (scale bar; 25 μm). (**B**) A similar pattern of Ki-67 expression (green) was detected in both immunofluorescent stained C4-2B (upper panels) and pASC tumor sections

(lower panels). (scale bar; 25 μm). (**C, D**) Immunohistochemical analysis of neoplastic markers p53 and Ras, respectively, in C4-2B and pASC tumor xenografts. Intense nuclear and cytoplasmic immunostaining for p53 (*arrow*) and Ras (*arrow*) is detected in tumor cells in both xenografts. Images shown are under low (scale bar; 50 μm) and high (scale bar; 20 μm) magnification. (**E**) Immunofluorescence microscopic analysis of vascular cell markers, von Willebrand factor (vWF) and α-smooth muscle actin (α-SMA), in C4-2B (upper panels) and pASC tumor xenografts (lower panels). Confocal images depict vWF (arrow) and α-SMA (arrowhead) stained with green and red fluorescence, respectively, in individual channels and merged images. DAPI stained nuclei are shown in blue. (scale bars, 20 μm).

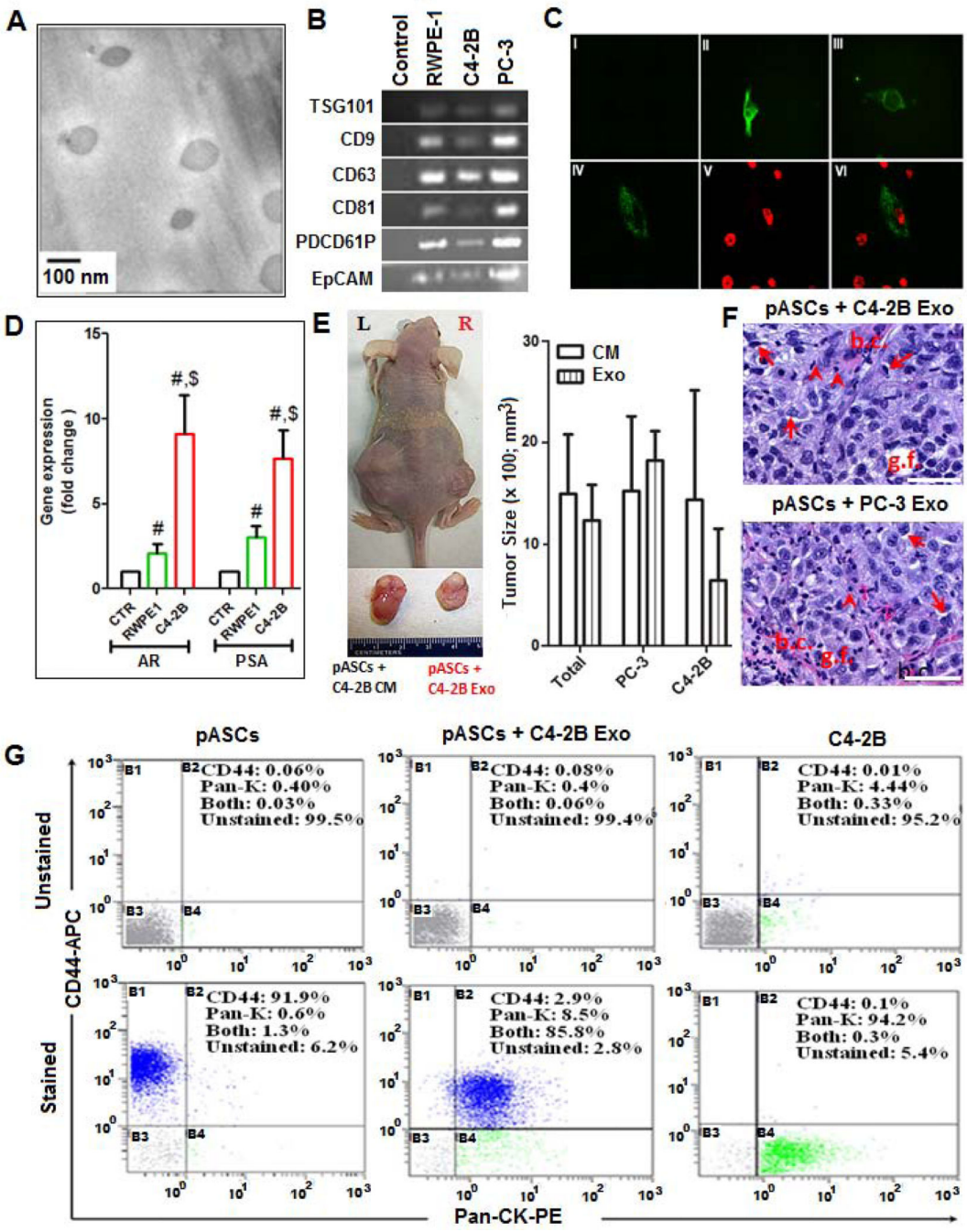


**Figure 4. Functional analysis of PC cell-derived exosomes in oncogenic transformation of pASCs**

(**A**): Morphologic characterization of exosomes isolated from CM of PC (C4-2B and PC-3) and normal prostate epithelial cells (RWPE-1) by Cryo-Scanning Electron Microscope (Cryo-TEM). Scale bar, 100 nm. (**B**) PCR analysis of tetraspanins (CD9, CD63, CD81, and PDCD61P) and the epithelial marker EpCAM in exosomes procured from RWPE-1 and PC cells. Supernatant of pelleted exosomes was used a control. (**C**) Cellular uptake of exosomes stained with PKH67, a fluorescent cell membrane dye (green). Confocal microscopy images of unstained (I) or stained exosomes derived from PC and RWPE-1 cells that were added to

cultured RWPE-1 cells (II), C4-2B cells (III), or to pASCs (IV) for 2 h. DAPI is shown in red (V) and the merged microphotograph (VI) depicts exosomes uptake by representative pASCs (400x). (**D**) Quantitative RT-PCR analysis of AR and PSA transcript levels in pASCs cultured in control medium (CTR) or treated with exosomes (Exo) procured from RWPE-1 (green bars) or C4-2B (red bars) cells. Data represent fold change in gene expression expressed as mean ± SEM of five different pASC isolates carried out in duplicates. The $ and # denote significance ($P<0.05$) in gene expression in pASCs treated with C4-2B derived Exo relative to CTR and RWPE-1 derived exosomes, respectively. (**E**) Tumor formation (left panel) by the same pASC isolate pretreated with either conditioned medium (CM) (left flank) or Exo (right flank) of C4-2B cells in nude mice. Relative tumor sizes are shown in the right panel and the bottom inset. (**F**) H&E staining of tumor sections of pASC tumors generated by Exo derived from either C4-2B cells (upper panel) and PC-3 cells (lower panel), showing prominent nucleoli, gland formation (g.f.), signet-ring morphology (*arrows*), scattered inflammatory cells (*arrowhead*), and thin capillaries (b.c.). Scale bar, 50 μM. (**G**) Single cell suspension (*passage 3*) of pASC tumor cells generated with C4-2B–derived Exo were stained for CD44 (APC) and pan-cytokeratin (pan-CK) (PE) and analyzed by flow cytometry. Näive pASCs and C4-2B cells were used as a control. The percentage of cells expressing CD44 (B1), pan-CK (B4), both (B2), and neither (B3) is shown in stained cells (lower panel) relative to control unstained cells (upper panel).

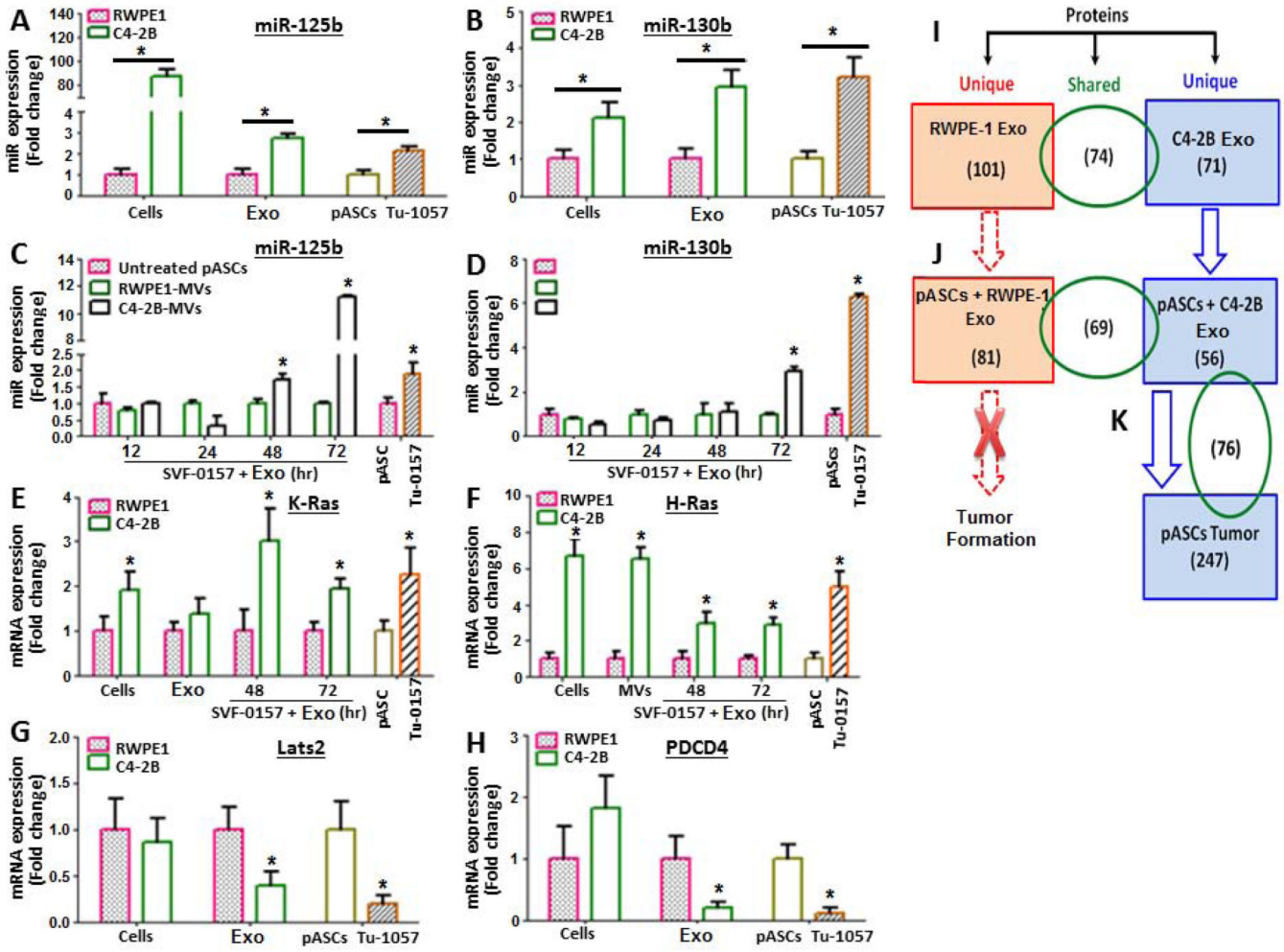


**Figure 5. Selective expression profile of oncomiRNAs, Ras family, and tumor suppressor transcripts in PC cell-derived exosomes and pASC tumor cells**

(**A, B**) Real-time PCR analysis of endogenous levels of miR-125b and miR-130b in normal prostate cells (RWPE-1), PC cells (C4-2B) and their associated exosomes (Exo), parental pASC (SVF-0157) and their derived ASC-tumor cells (Tu-0157). The Tu-0157 cells were isolated from primary tumor xenografts developed in mice by SVF-0157 cells treated with C4-2B–derived Exo. (**C, D**) Real-time PCR analysis of miR-125b and miR-130b transcripts, respectively, in pASCs (SVF-0157) treated for up to 72 h with Exo derived from RWPE-1 or C4-2B cells. (**E, F**) Constitutive and induced over-expression of K-Ras and H-Ras, respectively, in RWPE-1, C4-2B and their derived Exo, parental pASCs (SVF-0157), SVF-057 treated with Exo and their derived pASC tumor cells (Tu-0157). (**G, H**) Relative expression of tumor suppressors Lats2 and PDCD4, respectively, in RWPE-1, C4-2B and their derived Exo, and in parental pASCs (SVF-0157) and their transformed pASCs (Tu-0157). OncomiRNA expression was normalized to U6 snRNA (RNU6B), whereas K-Ras, H-Ras, Lats2, and PDCD4 transcript levels were normalized to GAPDH. Data is expressed as fold change relative to controls. All bars indicate SEM. *P*-values (<0.05) were calculated by Student's *t* test. (**I-K**) Summary of LC/MS/MS analyses of unique and shared peptide signature between Exo derived from C4-2B and RWPE-1 cells, parental pASCs

(SVF-0157) treated with Exo derived from RWPE-1 or C4-2B cells, and their derived pASC tumor cells (Tu-0157).

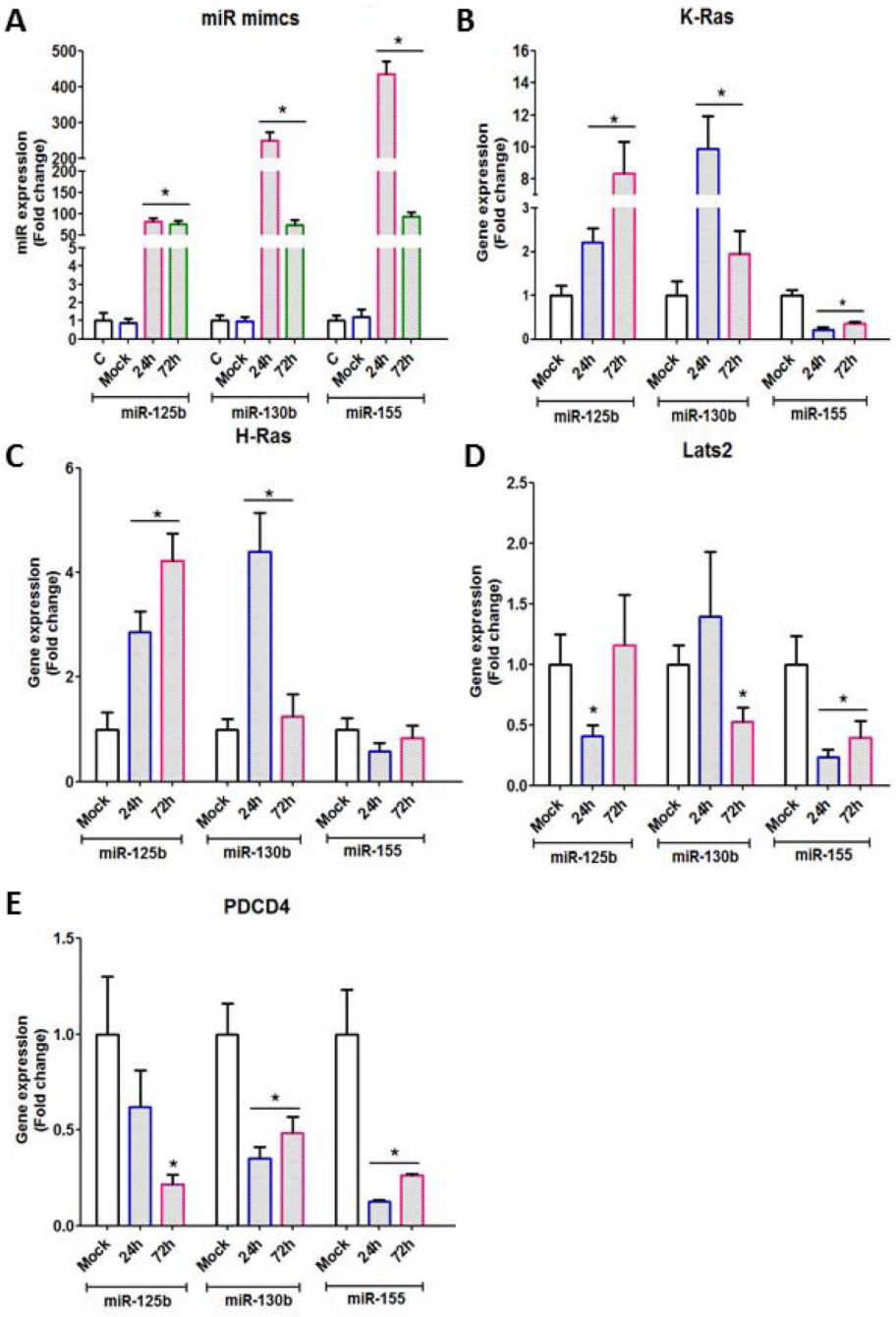


**Figure 6. OncomiRNAs functional analysis in miR mimic-transfected pASCs**

(**A**): Time course study depicting efficiency of expression ofmiR-125b, miR-130b and miR-155 in pASCs using miR mimics strategy. The miR mimics were overexpressed in pASCs and differential gene expression of K-Ras, H-Ras, Lats2 and PDCD4 was measured at 24hr and 72 hr by qRT-PCR analysis. Untransfected (c) and pASCs transfected with non-targeting miR mimics (mock) were used as controls. (**B-E**): Time course study to determine relative expression of K-ras, H-ras, Lats2 and PDCD4, respectively, in pASCs transfected

with oncomiRNA mimics or with non-targeting miR mimics (mock). *denotes significance at $P<0.05$ relative to mock transfected pASCs by student *t*-test.

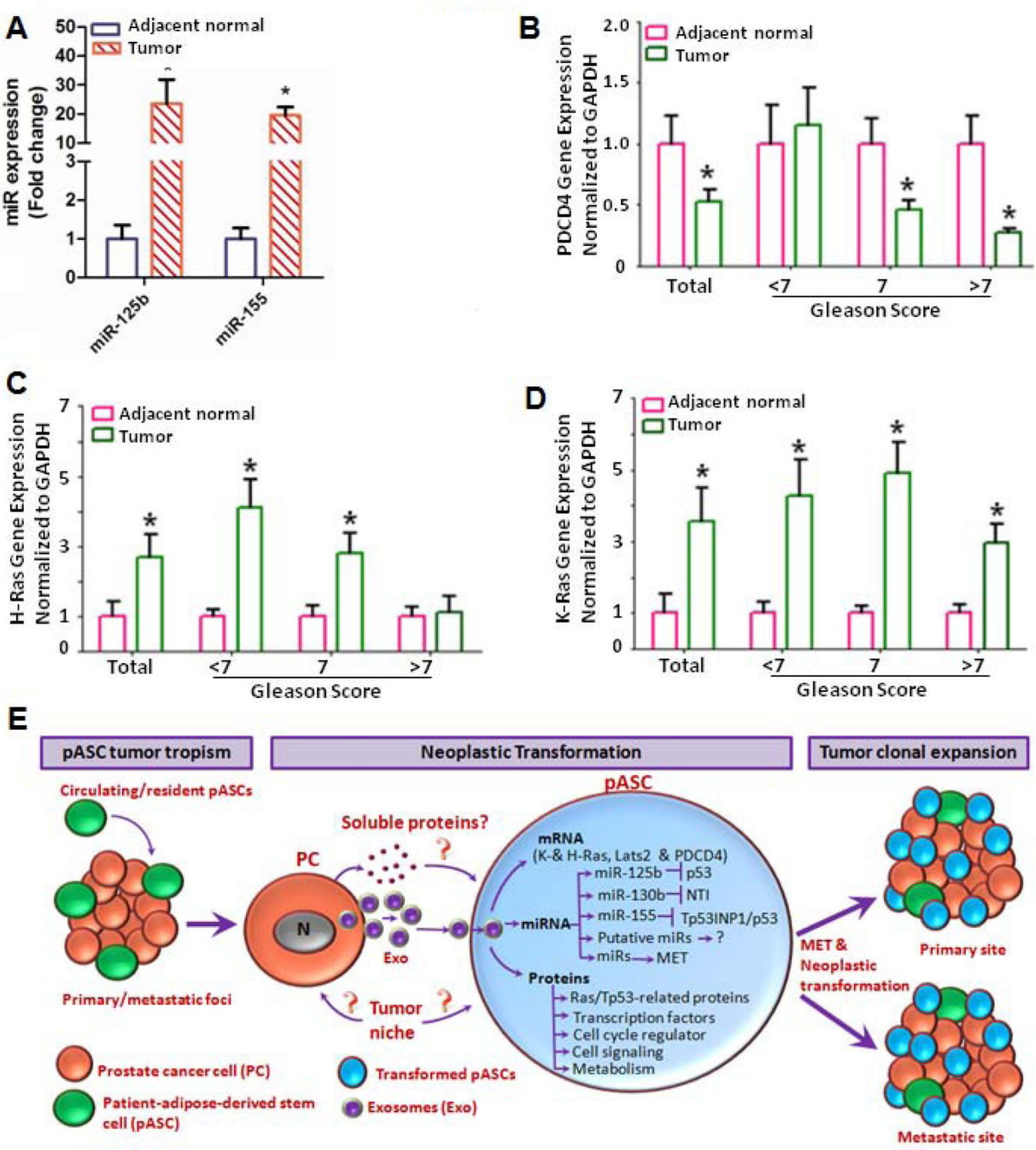


**Figure 7. Gene expression analysis of oncogenic factors and tumor suppressors in human microdissected prostate tumors and proposed model for tumor cell derived exosome-ASC interactions in cancer patients**

(**A**): Prostate tumor cells and adjacent normal glands were procured by laser capture microdissection (LCM) from snap-frozen PC tissues (Gleason score <7, 7 and >7; *n*=18) and analyzed for expression of miR-125b and miR-155 by qRT-PCR. OncomiRNA expression was normalized to U6 snRNA (RNU6B), and data is expressed as fold change relative to normal adjacent glands. *denotes significance at $P<0.001$ in tumor cells relative to adjacent normal glands by student *t*-test. (**B-D**): qRT-PCR analysis of PDCD4, H-Ras and K-Ras

gene expression, respectively, in microdissected prostate tumors in comparison adjacent normal glands. Data is presented as mean ± SEM in tumor cells relative to adjacent normal glands. *denotes significance ($P<0.05$) by student *t*-test. (**E**): Proposed model of mutual interactions between tumor tropic pASCs and PC cell-derived exosomes (Exo) in mediating tumor progression in cancer patients. The figure depicts selective recruitment of circulating and/or tissue resident ASCs to tumor microenvironment in cancer patients. The trafficking and functional activation of oncomiRNAs, Ras transcripts and Rab oncoproteins trigger mesenchymal-to-epithelial transition (MET) and neoplastic reprogramming in tumor recruited stem cells by tumor derived exosomes, which in turn promotes clonal expansion and disease progression at primary and/or metastatic sites in cancer patients.